Characterization of the admixed intermediate-spin complex bis(3-cyanopyridine)(octaethylporphinato)iron(III) perchlorate

Martin K. Safo, W. Robert Scheidt*
Department of Chemistry and Biochemistry, University of Notre Dame, Notre Dame, IN 46556 (U.S.A.)

Govind P. Gupta**
Department of Physics, Pennsylvania State University, State College, PA 16802 (U.S.A.)

Robert D. Orosz and **Christopher A. Reed***
Department of Chemistry, University of Southern California, Los Angeles, CA 90089-0744 (U.S.A.)

(Received January 17, 1991)

Abstract

The preparation of bis(3-cyanopyridine)(octaethylporphinato)iron(III) perchlorate is described. The molecular structure has been determined by an X-ray crystal structure determination. The centrosymmetric complex has coplanar axial pyridine ligands that are close to eclipsing an Fe–N_p bond ($\phi = 4°$). The average equatorial bond distance is 2.012(3) Å. The axial Fe–N(Py) bond distance is 2.269(6) Å. The complex has been further characterized by EPR and Mössbauer spectroscopy and temperature dependent magnetic susceptibility measurements between 1.8 and 300 K. The complex has an axial EPR spectrum with $g_\perp = 4.28$ and $g_\parallel = 1.97$. The Mössbauer spectrum in zero field at 77 K has an isomer shift of 0.38 mm/s and a quadrupole split doublet of 2.61 mm/s. The Mössbauer has also been studied in an applied magnetic field (6 T) at 4.2 K and fitted with a crystal field model. The structure and spin state of this compound serve to emphasize an emerging pattern in the relationship of axial ligand orientation (ϕ angles) and spin state. Crystal data: $[Fe(OEP)(3\text{-}CNPy)_2]ClO_4 \cdot 3CHCl_3$: $a = 10.463(7)$, $b = 24.805(26)$, $c = 11.661(4)$ Å, and $\beta = 109.60(6)°$, monoclinic, space group $P2_1/m$, $V = 2851.0$ Å^3, $Z = 2$, observed data = 3118, $R_1 = 0.099$, $R_2 = 0.102$.

Introduction

We [1–5] and others [6–8] have been investigating the effects of axially coordinated pyridine ligands on the physical properties of iron(III) porphyrinates. For octaethylporphyrin complexes, strongly and moderately basic pyridine ligands give low-spin ($S = 1/2$) iron(III) complexes [6, 7], while lower basicity pyridine ligands give a discrete admixed intermediate-spin state ($S = 3/2,5/2$) [2–4] or in one case, a thermal spin equilibrium complex ($S = 1/2 \rightleftharpoons 5/2$) [1, 8]. Understanding when a thermal spin equilibrium is favored over a discrete admixed intermediate-spin state has been an ongoing investigation in this laboratory. $[Fe(OEP)(3\text{-}ClPy)_2]ClO_4$ (pyridine ligand $pK_a = 2.83$) [9] is known to give both intermediate-spin and spin equilibrium states depending on the crystal lattice [1–3]. The complex $[Fe(OEP)(3,5\text{-}Cl_2Py)_2]ClO_4$ [4], with an even lower basicity ligand, was expected to give either a thermal spin equilibrium complex with greater high-spin fraction or a high-spin complex. However, the magnetic moment and the solid-state EPR spectrum of this complex identified it as a discrete admixed intermediate-spin state. Thus the line between an admixed intermediate-spin state and a thermal spin equilibrium, as modulated by axial ligand basicity, is not clearly defined.

Closely related to the basicity effects of the pyridine ligands in affecting the spin state is the axial ligand orientation with respect to the porphyrin coordinate system†. Bis-pyridine-ligated iron(III) porphyrinate complexes with small dihedral angles ($\phi < \sim 15°$) are incompatible with a low-spin state; the increased steric interaction at small ϕ angles is relieved by an elongation of the Fe–N(Py) bonds with the formation

*Authors to whom correspondence should be addressed.
**Present address: Department of Physics, Lucknow University, Lucknow 226007, India.

†The axial ligand orientation can be defined as the dihedral angle (ϕ) made by the axial ligand plane and the closest Fe–N_p bond vector. This orientation system was first defined by Hoard and co-workers [10].

0020-1693/91/$3.50

of an intermediate- or high-spin species. Thus, to form a low-spin iron(III) complex with pyridine ligands, ϕ must be relatively large. For the reported bis-pyridine complexes, those with intermediate or high basicity pyridine ligands have ϕ angles $>30°$, and the complexes are low spin [5, 6]. The complexes with low basicity pyridine ligands have very small ϕ angles and are admixed intermediate-spin state complexes [2–4]*.

To give more insight into how low basicity pyridine ligands affect the spin state of iron(III) porphyrinates, we have prepared the complex, $[Fe(OEP)(3\text{-}CNPy)_2]ClO_4$ (ligand $pK_a = 1.45$) [9]. We have characterized it by Mössbauer and EPR spectroscopy, magnetic susceptibility measurements and a single-crystal X-ray structure determination. The observed room temperature magnetic moment of 4.7 μ_B is similar to that found for the thermal spin equilibrium form of $[Fe(OEP)(3\text{-}ClPy)_2]ClO_4$ [1]. However, complexes [2, 11, 12] with discrete admixed intermediate-spin states are also known to have such large moments (4.4–5.5 μ_B). The EPR spectrum of the crystalline complex is axial with $g_\perp = 4.28$, a value consistent with a discrete admixed intermediate-spin state. The quadrupole splitting of 2.61–2.67 mm/s is much larger than those found for $S = 1/2$ iron(III) porphyrinates (1.6–2.3 mm/s) [13–16] and $S = 5/2$ complexes (0.6–1.3 mm/s) [13]. Thus both the EPR and Mössbauer data rule out a thermal spin equilibrium in $[Fe(OEP)(3\text{-}CNPy)_2]ClO_4$. The data are best interpreted in terms of a 'Maltempo' model, i.e. a quantum mechanically admixed spin state complex.

Experimental

Synthesis

$[Fe(OEP)(OClO_3)]$** was synthesized as described previously [11, 17]. $[Fe(OEP)(3\text{-}CNPy)_2]ClO_4$ was prepared from $[Fe(OEP)(OClO_3)]$ (210 mg, 0.31 mmol) and 3-cyanopyridine (100 mg, 0.96 mmol) dissolved in 25 ml chloroform. The solution was warmed for about 15 min, and the volume decreased to about 15 ml. The solution was filtered, layered with hexane and set in a refrigerator (9 °C) for crystallization. X-ray quality crystals formed after 5 days. UV–Vis spectra were recorded on a Perkin-Elmer Lambda 4C spectrometer, and IR spectra on a Perkin-Elmer 883 spectrometer. Samples for Mössbauer spectroscopy were prepared as Apiezon L grease mulls. Measurements were made at 77 and 4.2 K with and without applied magnetic field. EPR spectra were obtained at 77 K both in the solid-state and in CH_2Cl_2 frozen solution.

*The one exception is the thermal spin equilibrium form of $[Fe(OEP)(3\text{-}ClPy)_2ClO_4$ [1]. In this complex the ϕ angle is 41°.

**Abbreviations used: TPP and OEP, dianions of *meso*-tetraphenylporphyrin and octaethylporphyrin; 3-CNPy, 3-cyanopyridine; 3-ClPy, 3-chloropyridine; 3,5-Cl_2Py, 3,5-dichloropyridine; N_p, porphinato nitrogen; N_{ax}, axial nitrogen.

TABLE 1. Crystal data and intensity collection parameters[a]

Complex	$[Fe(OEP)(3\text{-}CNPy)_2]\text{-}ClO_4 \cdot 3CHCl_3$
Formula	$FeCl_{10}O_4N_8C_{51}H_{55}$
Formula weight (amu)	1254.4
Space group	$P2_1/m$
T (K)	118
a (Å)	10.463(7)
b (Å)	24.805(26)
c (Å)	11.661(4)
β (°)	109.60(6)
V (Å^3)	2851.04
Z	2
Scan technique	θ–2θ
Diffractometer	CAD4
Crystal dimensions (mm)	$0.2 \times 0.5 \times 0.1$
2θ Limits	4.0–56.80
Radiation	Mo Kα
Criterion for observation	$F_o > 2.0\sigma(F_o)$
No. observed data	3118
D_{obs} (g/cm^3)	1.44
D_{calc} (g/cm^3)	1.46
R_1	0.099
R_2	0.102

[a]D_{obs} obtained at 294 K and D_{calc} obtained at 118 K.

Magnetic data

Magnetic susceptibilities in the solid state were measured on finely ground samples packed into aluminium buckets. Data were taken from 1.8 to 300 K in a field of 2 and 10 kG on a SHE model 905 SQUID susceptometer. The data at 2 kG are displayed graphically in the text, see also 'Supplementary material'.

Structure determination

A crystal of $[Fe(OEP)(3\text{-}CNPy)_2]ClO_4$ was examined on an Enraf-Nonius CAD4 diffractometer at the ambient laboratory temperature of 293 K. Preliminary examination suggested a two-molecule monoclinic unit cell. However, attempts to measure intensity data failed due to rapid decomposition of the crystal, apparently from solvent loss. Data collection used a freshly prepared crystal of $[Fe(OEP)(3\text{-}CNPy)_2]ClO_4$ with dimensions of $0.2 \times 0.5 \times 0.1$ mm, mounted under a nitrogen gas cold stream (118 K) provided by a locally modified Syntex LT-1 low-temperature attachment on the diffractometer. Least-squares refinement of 25 centered reflections gave

TABLE 2. Fractional coordinates of [Fe(OEP)(3-CNPy)$_2$]ClO$_4$·3CHCl$_3$[a]

Atom	x	y	z
Fe	0.0000	0.0000	0.0000
N(1)	0.1559(5)	0.03480(24)	−0.0367(5)
N(2)	−0.0210(5)	−0.05284(24)	−0.1358(5)
N(3)	0.1417(6)	−0.05734(25)	0.1356(6)
N(4)	0.3478(8)	−0.0485(3)	0.5640(7)
C(a1)	0.2288(6)	0.0783(3)	0.0198(6)
C(a2)	0.2036(6)	0.02130(29)	−0.1299(6)
C(a3)	0.0512(6)	−0.05516(27)	−0.2144(6)
C(a4)	−0.1203(6)	−0.09166(29)	−0.1756(6)
C(b1)	0.3257(7)	0.0937(3)	−0.0377(6)
C(b2)	0.3100(6)	0.05837(28)	−0.1307(6)
C(b3)	−0.0026(7)	−0.09516(29)	−0.3076(7)
C(b4)	−0.1121(7)	−0.1171(3)	−0.2835(6)
C(m1)	0.1577(6)	−0.02058(28)	−0.2099(6)
C(m2)	0.2141(7)	0.1038(3)	0.1199(7)
C(11)	0.4228(8)	0.1397(3)	−0.0024(8)
C(21)	0.3884(8)	0.0557(3)	−0.2180(7)
C(31)	0.0473(8)	−0.1090(4)	−0.4094(8)
C(41)	−0.2110(9)	−0.1572(4)	−0.3580(8)
C(12)	0.5566(10)	0.1243(5)	0.0995(11)
C(22)	0.5121(8)	0.0200(4)	−0.1698(8)
C(32)	−0.0324(11)	−0.0851(6)	−0.5293(10)
C(42)	−0.3438(9)	−0.1310(6)	−0.4355(10)
C(1)	0.1790(9)	−0.1042(4)	0.1025(8)
C(2)	0.2625(12)	−0.1406(4)	0.1829(10)
C(3)	0.3094(10)	−0.1276(4)	0.3043(9)
C(4)	0.2702(7)	−0.0798(3)	0.3407(7)
C(5)	0.1869(6)	−0.0454(3)	0.2532(6)
C(6)	0.3172(8)	−0.0623(3)	0.4661(7)
C(7)	−0.4457(14)	0.2500	0.3766(13)
C(8)	0.0950(20)	0.2500	−0.2668(21)
C(9)	−0.118(6)	0.2301(12)	0.1268(28)
Cl(1)	0.4473(3)	0.2500	−0.3103(3)
O(1)	0.413(3)	0.2014(5)	−0.2832(23)
O(2)	0.5469(17)	0.2500	−0.3643(11)
O(3)	0.336(3)	0.2500	−0.426(3)
Cl(2)	−0.5672(4)	0.2500	0.2290(3)
Cl(3)	−0.34364(28)	0.19202(9)	0.39688(25)
Cl(4)	−0.0460(11)	0.2500	−0.4009(8)
Cl(5)	0.0975(6)	0.19228(18)	−0.1856(4)
Cl(6)	−0.2910(18)	0.2457(20)	0.0233(9)
Cl(7)	−0.0882(12)	0.2396(5)	0.2688(9)
Cl(8)	−0.0049(15)	0.2369(6)	0.0606(11)

[a]c.s.d.s. of the least significant digits are given in parentheses.

the cell constants reported in Table 1. The systematic absences are consistent with the space group $P2_1$ or $P2_1/m$.

Four standard reflections were measured during data collection; there were no significant fluctuations in their intensities. Intensity data were reduced with the profile fitting algorithm of Blessing [18]. A summary of crystal data, intensity collection parameters and least-squares refinement parameters of [Fe(OEP)(3-CNPy)$_2$]ClO$_4$ are reported in Table 1. Data were collected to a maximum of $2\theta = 56.80$,

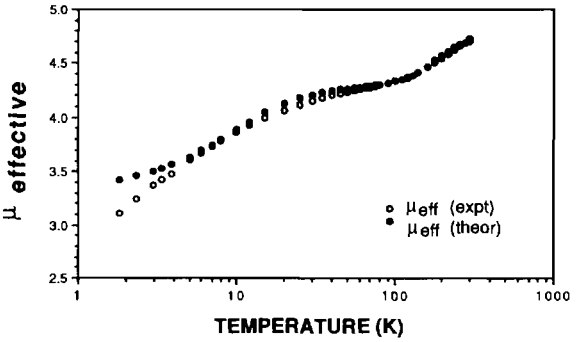

Fig. 1. Experimental and calculated values of the effective magnetic moment vs. temperature for [Fe(OEP)(3-CNPy)$_2$]ClO$_4$·1.5CHCl$_3$. The calculated values were obtained by using the parameters $g_\perp = 4.48$ and $\zeta = 150$ cm^{-1}.

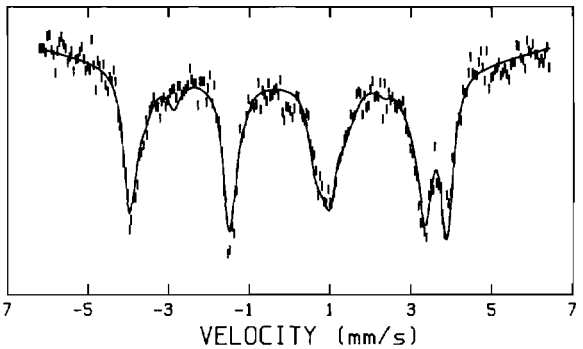

Fig. 2. Mössbauer spectrum of [Fe(OEP)(3-CNPy)$_2$]ClO$_4$ recorded at 4.2 K in a 6 T field.

and all data with $F_o \geq 2.0\sigma(F_o)$ were retained as observed and used in all subsequent least-squares refinement. The structure was solved in the centrosymmetric space group $P2_1/m$ using the direct methods program MULTAN [19]. All subsequent developments of structure solution and refinement were consistent with this choice. Atomic form factors were taken from ref. 20a; real and imaginary corrections for anomalous dispersion in the form factor of the iron and chlorine atoms were from ref. 20b; scattering factors for hydrogen were from ref. 20c; all calculations were performed on a VAX 3200 computer. The E map and subsequent difference Fourier syntheses led to the location of all atoms including one perchlorate anion and three chloroform molecules. The structure consists of one-half of a [Fe(OEP)(3-CNPy)$_2$]ClO$_4$ molecule in the asymmetric unit with required inversion symmetry. The perchlorate has a mirror plane passing through the chlorine and two oxygen atoms. Two of the chloroform molecules also have mirror planes passing through the carbon and one chlorine atom. The third chloroform solvent molecule was disordered in two positions. The carbon lies near a mirror plane and is about 0.9 Å from its mirror image. There are six

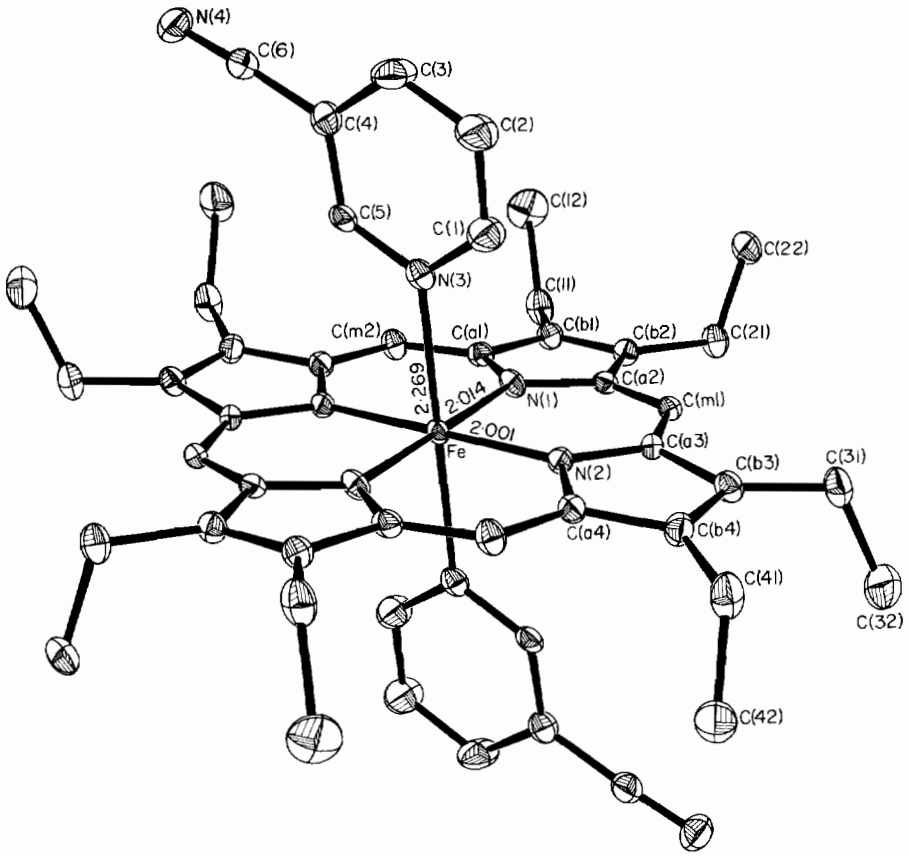

Fig. 3. ORTEP diagram of $[Fe(OEP)(3\text{-}CNPy)_2]ClO_4$. The atom labeling scheme for the crystallographic unique atoms and the bond distances in the coordination group are also shown. 50% probability surfaces are shown.

chlorine atoms associated with the two carbon atom positions. Occupancies of 0.5 were used for all atoms in the disordered chloroform. Several cycles of difference Fourier syntheses led to the location of most hydrogen atoms. The hydrogen atom positions were idealized and included in subsequent cycles of least-squares as fixed contributors (C–H = 0.95 Å, B(H) = B(C) + 1.0 Å) Final cycles of least-squares refinements were carried out with anisotropic temperature factors for all heavy atoms. Final atomic coordinates are listed in Table 2. See also 'Supplementary material'.

Results

$[Fe(OEP)(3\text{-}CNPy)_2]ClO_4$ has been characterized by IR, UV–Vis, EPR and Mössbauer spectroscopy, magnetic susceptibility measurements and a single-crystal X-ray structure determination. The magnetic susceptibility was measured both at 2 and 10 kG in the temperature range of 1.8–300 K. The solid sample is known to readily lose solvent of crystallization and 1.5 chloroform molecules of solvation were used for the molecular weight and diamagnetic correction calculations. The data are shown graphically in Fig. 1. A logarithmic temperature scale was chosen to best show the rapid decrease of the moment at low temperature. The 2 and 10 kG data sets are similar within experimental error. The magnetic moment climbs sharply from 3.11 μ_B at 1.8 K and levels at 100 K (4.33 μ_B), and then climbs slowly to 4.72 μ_B at 300 K. This behavior is typical of a quantum mechanically admixed intermediate-spin state [2, 3, 4, 11, 21, 22, 23].

The data shown in Fig. 1 were compared with the Maltempo [24] model by use of the Hamiltonian

$$\mathscr{H}_{el} = \Delta + \sum_i \zeta \mathbf{l}_i s_i + 2\beta \mathbf{HS} \qquad (1)$$

where Δ is the energy gap between the $S = 3/2$ and 5/2 spin states, the second term is the spin–orbit interaction with ζ as its one-electron-coupling constant (summation over i is extended over all five 3d electrons of the ferric ion), and the last term is the Zeeman interaction of the electronic spin S ($= \Sigma s_i$) with the external field H.

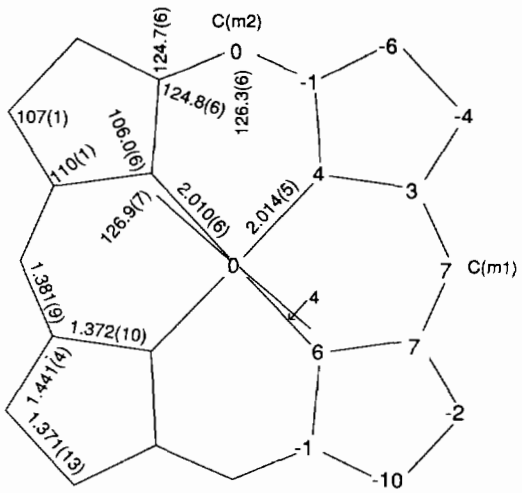

Fig. 4. Formal diagram of the porphinato core in $[Fe(OEP)(3\text{-}CNPy)_2]ClO_4$. Deviations of each unique atom from the mean plane of the core (in units of 0.01 Å) are shown. Averaged values for the chemically unique bond distances and angles in the core are shown. The orientation of the axial ligands with the closest Fe–N_p vector (angle ϕ) are shown. Individual values of the Fe–N_p bond distances are shown.

TABLE 3. Bond distances in $[Fe(OEP)(3\text{-}CNPy)_2]ClO_4 \cdot 3CHCl_3$[a]

Type	Length (Å)	Type	Length (Å)
Fe–N(1)	2.014(5)	C(21)–C(22)	1.512(12)
Fe–N(2)	2.010(6)	C(31)–C(32)	1.489(16)
Fe–N(3)	2.269(6)	C(41)–C(42)	1.526(15)
N(1)–C(a1)	1.358(10)	C(1)–C(2)	1.381(14)
N(1)–C(a2)	1.381(8)	C(2)–C(3)	1.372(15)
N(2)–C(a3)	1.372(8)	C(3)–C(4)	1.368(14)
N(2)–C(a4)	1.378(9)	C(4)–C(5)	1.391(11)
N(3)–C(1)	1.324(11)	C(4)–C(6)	1.445(12)
N(3)–C(5)	1.326(10)	C(6)–N(4)	1.130(11)
C(a1)–C(b1)	1.443(9)	Cl(1)–O(1)	1.325(11)
C(a1)–C(m2)	1.380(10)	Cl(1)–O(1)′	1.325(11)
C(a2)–C(b2)	1.447(9)	Cl(1)–O(2)	1.386(13)
C(a2)–C(m1)	1.371(10)	Cl(1)–O(3)	1.458(24)
C(a3)–C(b3)	1.439(10)	C(7)–Cl(2)	1.763(16)
C(a3)–C(m1)	1.393(9)	C(7)–Cl(3)	1.760(8)
C(a4)–C(b4)	1.436(10)	C(8)–Cl(4)	1.753(22)
C(a4)–C(m2)′	1.379(9)	C(8)–Cl(5)	1.712(14)
C(b1)–C(b2)	1.362(10)	C(9)–Cl(9)″	0.99(6)
C(b3)–C(b4)	1.380(10)	C(9)–Cl(6)	1.85(5)
C(b1)–C(11)	1.489(11)	C(9)–Cl(6)″	1.91(6)
C(b2)–C(21)	1.507(9)	C(9)–Cl(7)	1.60(3)
C(b3)–C(31)	1.488(10)	C(9)–Cl(7)″	1.75(3)
C(b4)–C(41)	1.488(12)	C(9)–Cl(8)	1.62(5)
C(11)–C(12)	1.550(15)	C(9)–Cl(8)″	1.81(6)

[a]e.s.d.s. of the least significant digits are given in parentheses. Primed and unprimed symbols denote a pair of atoms related by an inversion center at iron. Double primed and unprimed symbols denote a pair of atoms related by a mirror plane.

The energy separation Δ is related to the transverse gyromagnetic ratio $g_\perp$ of the lowest doublet, $S_z = \pm 1/2$, by

$$\Delta = \pm\zeta\left[-\frac{24(g_\perp - 5)^2}{5(g_\perp - 6)(g_\perp - 4)}\right]^{1/2} \quad (2)$$

where the lower sign applies for $g_\perp < 5$. Normally, $g_\perp$ is proportional to the magnetic splitting of the ground doublet and may be directly measured by EPR. Moreover it can also be considered as a parameter indicating the percentage of the spin state $S = 3/2$ in the admixed spin state. The value of $g_\perp$ is linearly related to the percentage [24] of $S = 3/2$ character with boundary values 0 and 100% corresponding to $g_\perp = 6$ and 4, respectively. Theoretical values of magnetic moment (μ_{eff}) obtained by using the parameters $g_\perp = 4.48$ and $\zeta = 150\ cm^{-1}$ are shown in Fig. 1. The fitted $g_\perp$ value of 4.48, however, is higher than the value found for the EPR spectrum ($g_\perp$ of 4.28), or the 4.23 value obtained from the Mössbauer fit.

The EPR spectra of both solid and frozen solution (CH_2Cl_2) are axial. The EPR spectrum of the solid has $g_\perp = 4.28$ and $g_\parallel = 1.97$; the frozen solution spectrum has the same g values within experimental error.

The Mössbauer spectrum of the complex has been determined at both 4.2 and 77 K. The values of δ and ΔE_q at 77 K are 0.38 and 2.61 mm/s. At 4.2 K and no magnetic field the values are 0.36 and 2.67 mm/s, respectively. In an applied magnetic field of 6 T at 4.2 K, $\delta = 0.42$ mm/s and $\Delta E_q = 2.67$ mm/s. The spectrum in an applied magnetic field is shown in Fig. 2. The value of δ is independent of temperature within experimental errors. There is a very small increase in the value of ΔE_q with temperature. A fit to the Mössbauer data gives $g_\perp = 4.23$ closely comparable with the experimental EPR value.

The molecular structure of $[Fe(OEP)(3\text{-}CNPy)_2]ClO_4$ is shown in the ORTEP diagram in Fig. 3. The numbering scheme for the crystallographically unique atoms and bond distances around the iron atom are also displayed. Average values for the chemically equivalent bond distances and angles in the core of the complex are shown in Fig. 4. The number in parentheses following each averaged value is the estimated standard deviation calculated on the assumption that the individual values are all drawn from the same population. Individual values of the Fe–N_p bond distances and the dihedral angle made by the axial ligand plane are also shown in Fig. 4. Figure 4 also shows the displacement of the crystallographically unique atom from the mean plane

TABLE 4. Bond angles in $[Fe(OEP)(3\text{-}CNPy)_2]ClO_4 \cdot 3CHCl_3$[a]

Type	Value (°)	Type	Value (°)
N(1)–Fe–N(2)	89.68(22)	C(b1)–C(b2)–C(21)	128.2(6)
N(1)–Fe–N(2)′	90.32(22)	C(a3)–C(b3)–C(b4)	105.0(6)
N(1)–Fe–N(3)	88.25(21)	C(a3)–C(b3)–C(31)	127.4(6)
N(2)–Fe–N(3)	90.77(13)	C(b4)–C(b3)–C(31)	127.5(6)
Fe–N(1)–C(a1)	126.9(4)	C(a4)–C(b4)–C(b3)	107.6(6)
Fe–N(1)–C(a2)	126.5(5)	C(a4)–C(b4)–C(41)	124.9(6)
C(a1)–N(1)–C(a2)	106.4(5)	C(b3)–C(b4)–C(41)	127.4(6)
Fe–N(2)–C(a3)	128.0(4)	C(a2)–C(m1)–C(a3)	125.9(6)
Fe–N(2)–C(a4)	126.3(4)	C(a1)–C(m2)–C(a4)′	126.7(6)
C(a3)–N(2)–C(a4)	105.5(5)	C(b1)–C(11)–C(12)	112.3(8)
Fe–N(3)–C(1)	122.3(5)	C(b2)–C(21)–C(22)	111.6(6)
Fe–N(3)–C(5)	120.2(5)	C(b3)–C(31)–C(32)	114.9(7)
C(1)–N(3)–C(5)	117.4(7)	C(b4)–C(41)–C(42)	112.2(9)
N(1)–C(a1)–C(b1)	110.7(6)	N(3)–C(1)–C(2)	123.8(8)
C(b1)–C(a1)–C(m2)	124.5(7)	C(1)–C(2)–C(3)	118.2(8)
N(1)–C(a1)–C(m2)	124.8(6)	C(2)–C(3)–C(4)	118.8(8)
N(1)–C(a2)–C(b2)	109.4(6)	C(3)–C(4)–C(5)	119.0(7)
C(b2)–C(a2)–C(m2)	124.9(6)	N(3)–C(5)–C(4)	122.7(7)
N(1)–C(a2)–C(m1)	125.7(6)	O(1)–Cl(C)–O(1)	131(1)
N(2)–C(a3)–C(b3)	111.7(5)	O(1)–Cl(C)–O(2)	114.4(7)
C(b3)–C(a3)–C(m1)	124.0(6)	O(1)–Cl(C)–O(3)	92(2)
N(2)–C(a3)–C(m1)	124.2(6)	O(2)–Cl(C)–O(3)	94(2)
N(2)–C(a4)–C(b4)	110.0(6)	Cl(3)–C(7)–Cl(3)″	109.6(7)
C(b4)–C(a4)–C(m2)′	125.3(6)	Cl(3)–C(7)–Cl(2)	109.7(5)
N(2)–C(a4)–C(m2)′	124.7(6)	Cl(3)′–C(7)–Cl(2)	109.7(5)
C(a1)–C(b1)–C(b2)	106.5(6)	Cl(5)–C(8)–Cl(5)″	114(1)
C(a1)–C(b1)–C(11)	126.5(7)	Cl(5)–C(8)–Cl(4)	110.2(8)
C(b2)–C(b1)–C(11)	127.0(6)	Cl(5)′–C(8)–Cl(4)	110.2(8)
C(a2)–C(b2)–C(b1)	107.0(6)	Cl(7)–C(9)–Cl(6)	116.9(27)
C(a2)–C(b2)–C(21)	124.8(6)	Cl(7)–C(9)–Cl(8)	124(3)
		Cl(8)–C(9)–Cl(6)	112.2(19)

[a]e.s.d.s. of the least significant digits are given in parentheses. Primed and unprimed symbols denote a pair of atoms related by an inversion center at iron. Double primed and unprimed symbols denote a pair of atoms related by a mirror plane.

TABLE 5. Bond parameters and axial ligand orientation of pyridine ligands in intermediate-spin Fe(III) porphyrinates

Complex	$M\text{–}N_p$[a]	M–N(Py)[a]	ϕ[b]	$\Delta\phi$[b, c]	Reference
$[Fe(OEP)(3\text{-}CNPy)_2]ClO_4$	2.012(3)	2.269(6)	4.0	0	this work
$[Fe(OEP)(3\text{-}ClPy)_2]ClO_4$[d]					2
molecule 1	2.003(1)	2.314(8)	5.7, 7.0	1	
molecule 2	2.008(8)	2.303(27)	11.5, 13.9	2.5	
$[Fe(OEP)(3\text{-}ClPy)_2]ClO_4 \cdot CHCl_3$	2.006(8)	2.304(27)	8.7, 6.1	2.6	3
$[Fe(OEP)(3\text{-}ClPy)]ClO_4$	1.979(6)	2.126(5)	41.1	NA[e]	3
$[Fe(OEP)(3,5\text{-}ClPy)_2]ClO_4$	1.994(10)	2.347(27)		0	4

[a]Value in Å. [b]Value in deg. [c]Relative orientation of two axial ligand planes. A value of 0 indicates planes required to be parallel by crystallographic symmetry. [d]Two independent molecules. [e]Not applicable.

of the 24-atom core (in units of 0.01 Å) in the complex. The complex has a modestly ruffled porphinato core. Individual bond distances and angles are listed in Tables 3 and 4. Average $Fe\text{–}N_p$ and $F\text{–}N_{ax}$ bond distances are 2.012(3) and 2.269(6) Å. Table 5 gives tabulated average values of $Fe\text{–}N_p$ and $Fe\text{–}N_{ax}$ bond distances for other intermediate spin state complexes. Also shown in the Table are the dihedral angle ϕ and the relative interplanar angles of the complexes.

Discussion

The effective magnetic moment at room temperature of 4.7 μ_B is significantly higher than that of a pure $S=3/2$ system. The value is similar to the observed room-temperature magnetic moment found for the thermal spin equilibrium complex, $[Fe(OEP)(3\text{-}ClPy)_2]ClO_4$ [1, 8]. However, other complexes with admixed intermediate-spin states are also found to have large moments [2, 11, 12]. Typical of an admixed intermediate-spin state, the magnetic moment climbs up sharply from 3.11 μ_B at 1.8 K and levels at 100 K at 4.33 μ_B, and then climbs up slowly to reach 4.72 μ_B at 300 K. The calculated fit to the experimental data is quite good except at the very lowest temperatures ($T<4$ K). Such deviations suggest magnetic coupling between iron porphyrinates. In a number of cases, the coupling model involved pairs of molecules [21, 25]. In the present case, there are no close interactions between pairs. A mean-field model, such as the one used for $[Fe(TPP)(FSbF_5)]\cdot C_6H_5F$ [22], might be appropriate. We have not attempted such a fit for $[Fe(OEP)(3\text{-}CNPy)_2]ClO_4$ because of the difficulties with defining the precise molecular weight for the crystalline material. The Mössbauer consists of a quadrupole doublet, with the right-hand line very broad. The quadrupole splitting is larger than those found for $S=1/2$ and 5/2 iron(III) porphyrinates. It should be noted that the value of ΔE_q (2.61–2.69 mm/s) is lower than any reported for an admixed intermediate-spin state complex, except $[Fe(OEP)(3\text{-}ClPy)_2]ClO_4$ [2], where ΔE_q was 2.5–2.7 mm/s. The data from both the susceptibility measurements and Mössbauer indicate the complex to have an admixed intermediate-spin state. The experimental value of $g_\perp$ from the EPR spectrum conclusively indicates an admixed intermediate-spin state.

The equatorial Fe–N_p bond distances of $[Fe(OEP)(3\text{-}CNPy)_2]ClO_4$ are the largest found among the other bis(pyridine) admixed intermediate-spin state complexes [2–4]. For a high-spin complex, the $d_{x^2-y^2}$ orbital is fully populated, which leads to a significant increase in the Fe–N_p bond distances. The admixed intermediate-spin state has only a partial population of this orbital, and consequently the Fe–N_p bond length in these systems is shorter (1.994(10)–2.008(8) Å). The axial Fe–N(Py) bond distance in $[Fe(OEP)(3\text{-}CNPy)_2]ClO_4$ of 2.269(6) Å is shorter than the 2.303(27)–2.347(27) Å range found in the other admixed intermediate-spin state species.

The present complex, $[Fe(OEP)(3\text{-}CNPy)_2]ClO_4$, confirms what is becoming an established pattern for solid-state (octaethylporphinato)iron(III) bis(pyridinates). Low-spin complexes require reasonable pyridine basicity and ϕ angles close to 45°. Intermediate-spin complexes arise with lower basicity pyridines and all have low ϕ angles. There does not seem to be any reason why intermediate-spin complexes with large ϕ angles should not exist. However, the only case of a large ϕ angle complex that is not low spin is the high-spin/low-spin thermal equilibrium species $[Fe(OEP)(3\text{-}ClPy)_2]ClO_4$ [1]. Here, of course, the ligand orientation is apparently trapped at high ϕ by crystal packing forces. It remains a challenge to understand this phenomenon and to develop a greater synthetic control of the subtle features which dictate the particular ϕ angle.

Supplementary material

Table S1, complete susceptibility data; Table S2, anisotropic thermal parameters; Table S3, fixed hydrogen atom positions; and Table S4, a listing of structure factors ($\times 10$) are available from the authors on request.

Acknowledgement

We thank the National Institutes of Health for support of this research under Grants GM-38401 (W.R.S.), HL-16860 to George Lang, and GM-23851 (C.A.R.).

References

1 W. R. Scheidt, D. K. Geiger and K. J. Haller, *J. Am. Chem. Soc., 104* (1982) 495.
2 W. R. Scheidt, D. K. Geiger, R. G. Hayes and G. Lang, *J. Am. Chem. Soc., 105* (1983) 2625.
3 W. R. Scheidt, D. K. Geiger, Y. J. Lee, C. A. Reed and G. Lang, *Inorg. Chem., 26* (1987) 1039.
4 W. R Scheidt, S. R. Osvath, Y. J. Lee, C. A. Reed, B. Shaevitz and G. P. Gupta, *Inorg. Chem., 28* (1989) 1591.
5 M. K. Safo, G. P. Gupta, F. A. Walker and W. R. Scheidt, *J. Am. Chem. Soc.*, in press.
6 D. Inniss, S. M. Soltis and C. E. Strouse, *J. Am. Chem. Soc., 110* (1988) 5644.
7 F. A. Walker, D. Reis and V. L. Balke, *J. Am. Chem. Soc., 106* (1984) 6888.
8 H. A. O. Hill, P. D. Skyte, J. W. Buchler, H. Leuken, M. Tonn, A. K. Gregson and G. Pellizer, *J. Chem. Soc., Chem. Commun.*, (1979) 151.
9 A. Albert, in A. R. Katritzky (ed.), *Physical Methods in Heterocyclic Chemistry*, Vol. I, Academic Press, New York, 1963, p. 68.
10 D. M. Collins, R. Countryman and J. L. Hoard, *J. Am. Chem. Soc., 94* (1972) 2066.
11 D. H. Dolphin, J. R. Sams and T. B. Tsin, *Inorg. Chem., 16* (1977) 711.

12 T. Mashiko, C. A. Reed, M. E. Kastner, K. J. Haller and W. R. Scheidt, *J. Am. Chem. Soc., 103* (1981) 5758.
13 J. R. Sams and T. B. Tsin, in D. Dolphin (ed.), *The Porphyrins,* Vol. IV, Academic Press, New York, 1979, p. 425.
14 L. M. Epstein, D. K. Straub and C. Maricondi, *Inorg. Chem., 6* (1967) 1720.
15 L. Bullard, R. M. Panayappan, A. N. Thorpe and P. Hambright, *Bioinorg. Chem., 3* (1974) 495.
16 D. K. Straub and W. M. Connor, *Ann. N.Y. Acad. Sci., 206* (1973) 383.
17 H. Ogoshi, E. Watanabe and Z. Yoshida, *Chem. Lett.,* (1973) 989.
18 R. H. Blessing, *Cryst. Rev., 1* (1987) 3.
19 P. Main, S. E. Hull, L. Lessinger, G. Germain, J.-P. Declerq and M. M. Woolfson, *MULTAN78,* a system of computer programs for the automatic solution of crystal structures from X-ray diffraction data, Universities of York, U.K. and Louvain, Belgium, 1978; R. L. Lapp and R. A. Jacobson, *ALLS,* a generalized crystallographic least-squares program, National Technical Information Services *IS-4708 UC-4,* Springfield, VA, U.S.A.; W. R. Busing, K. O. Martin and H. A. Levy, *ORFFE, Rep. ORNL-TM-306,* Oak Ridge National Laboratory, Oak Ridge, TN, U.S.A., 1964; C. K. Johnson, *ORTEPII, Rep. ORNL-5138,* Oak Ridge National Laboratory, Oak Ridge, TN, U.S.A., 1976.
20 (a) D. T. Cromer and J. B. Mann, *Acta Crystallogr., Sect. A, 24* (1968) 321; (b) D. T. Cromer and D. J. Liberman, *J. Chem. Phys., 53* (1970) 1891; (c) R. F. Stewart, E. R. Davidson and W. T. Simpson, *J. Chem. Phys., 42* (1965) 3175.
21 G. P. Gupta, G. Lang, W. R. Scheidt, D. K. Geiger and C. A. Reed, *J. Chem. Phys., 85* (1986) 5212.
22 G. P. Gupta, G. Lang, C. A. Reed, K. Shelly and W. R. Scheidt, *J. Chem. Phys., 86* (1987) 5288.
23 G. P. Gupta, G. Lang, Y. J. Lee, W. R. Scheidt, K. Shelly and C. A. Reed, *Inorg. Chem., 26* (1987) 3022.
24 M. M. Maltempo and T. H. Moss, *Q. Rev. Biophys., 9* (1976) 181.
25 G. P. Gupta, G. Lang, W. R. Scheidt, D. K. Geiger and C. A. Reed, *J. Chem. Phys., 83* (1985) 5945.